Advanced Robotics

ISSN: 0169-1864 (Print) 1568-5535 (Online) Journal homepage: https://www.tandfonline.com/loi/tadr20

# An uncertainty compensator for robust control of wheeled mobile robots

Aliasghar Arab & Mohammad Mehdi Fateh

**To cite this article:** Aliasghar Arab & Mohammad Mehdi Fateh (2015) An uncertainty compensator for robust control of wheeled mobile robots, Advanced Robotics, 29:20, 1303-1313, DOI: 10.1080/01691864.2015.1059366

**To link to this article:** https://doi.org/10.1080/01691864.2015.1059366

Published online: 07 Oct 2015.

Submit your article to this journal

Article views: 197

View related articles

View Crossmark data

Citing articles: 7 View citing articles

Full Terms & Conditions of access and use can be found at
https://www.tandfonline.com/action/journalInformation?journalCode=tadr20

*Advanced Robotics*, 2015
Vol. 29, No. 20, 1303–1313, http://dx.doi.org/10.1080/01691864.2015.1059366

Taylor & Francis
Taylor & Francis Group

FULL PAPER

# An uncertainty compensator for robust control of wheeled mobile robots

Aliasghar Arab*, and Mohammad Mehdi Fateh

*Department of Electrical and Robotic Engineering, Shahrood University, Shahrood, Iran*

(*Received 3 October 2014; revised 8 March 2015; accepted 20 May 2015*)

This paper proposes an uncertainty compensator to design a novel robust control for mobile robots with dynamic and kinematic uncertainties. A novel gradient-based adaptive fuzzy estimator is developed to compensate uncertainties with minimum required feedback signals. As a novelty, the proposed approach uses the tracking error and its first time derivative to form the estimation error of uncertainty, and guarantees that both the estimation error and tracking error converge asymmetrically to ignorable value. Advantages of the proposed robust control are simplicity in design, robustness against uncertainties, guaranteed stability, and good control performance. The control approach is verified by stability analysis. Simulation results and experimental results illustrate the effectiveness of the proposed control. Experimental evaluation of the proposed controller is expressed for two different low-cost nonholonomic wheeled mobile robots. The proposed control design is compared with an adaptive control approach to confirm the superiority of the proposed approach in terms of precision, simplicity of design, and computations.

**Keywords:** wheeled mobile robot; robust control; system uncertainty; adaptive fuzzy; gradient descent

## 1. Introduction

Dynamics of a mobile robot is nonlinear, uncertain, and multivariable. A precise tracking control in the presence of uncertainties is still an open question. The conventional robust control for the mobile robots faces some challenges such as the complexity of design, determining the bounding functions, chattering problem, effects of actuator dynamics, and computational burden. The proposed control design in this paper differs from previous robust control approaches which are complex due to using the torque control strategy. For example, one can address $H_\infty$ control,[1] sliding mode control,[2] adaptive control,[3] adaptive sliding mode control,[4] Lyapunov-based design of robust back-stepping controller,[5] robust continuous control,[6] and robust adaptive control.[7] Alternatively, intelligent control has become interesting for controlling complex systems by function approximation. There are valuable research works in this field such as adaptive neural control,[8] adaptive fuzzy control,[9] and fuzzy neural control [10] to name a few. All the mentioned methods are based on the torque control strategy. Robust control design for robot manipulators and mobile robots is more straightforward and precise when controller is designed using voltage strategy.[11,12] The torque control strategy is nonlinear, multivariable, and computationally extensive. In addition, the dynamics of robot's motors are excluded from the control problem, whereas they become dominant in high-velocity and high-precise applications. It has been shown that the dynamics of actuators should be taken into consideration to ensure a reliable and meaningful control performance.[11] The torque commands are assumed as inputs of the robotic system; however, the robot is driven by motors with voltage inputs in practice. Therefore, giving the voltage commands as the control inputs is realized to be more practical than the torque commands.

In addition, because of nonholonomic constraints, a main trend in the control of the wheeled robots is the use of two control loops, namely the kinematic control and the torque control. Some of control approaches such as ones presented in [4,8,13] have used the mentioned structure to control a wheeled robot. The purpose of the kinematic controller is to produce the velocity output for the robot to make the tracking error converges to zero. A torque controller is designed based on the system dynamics such that the velocity of the mobile robot converges to the generated desired velocity by the kinematic controller. The early approach proposed for the kinematic controller is the back-stepping control.[14] To improve its performance, adaptive kinematic control,[15] fuzzy control,[16] and neural network [17] were developed. In addition, input–output feedback linearizing control was proposed by researchers to simplify the controller structure by omitting the kinematic loop.[13,18]

Approximation methods were used in both kinematic loop [8] and dynamic loop [19] using neural networks

*Corresponding author. Email: aliarb1990@gmail.com
Recently, I graduated in MSc of Control Engineering and jointed to Department of Mechanical and Aerospace Engineering, Rutgers University, as a visiting student. This paper is related to my MSc thesis.

© 2015 Taylor & Francis and The Robotics Society of Japan

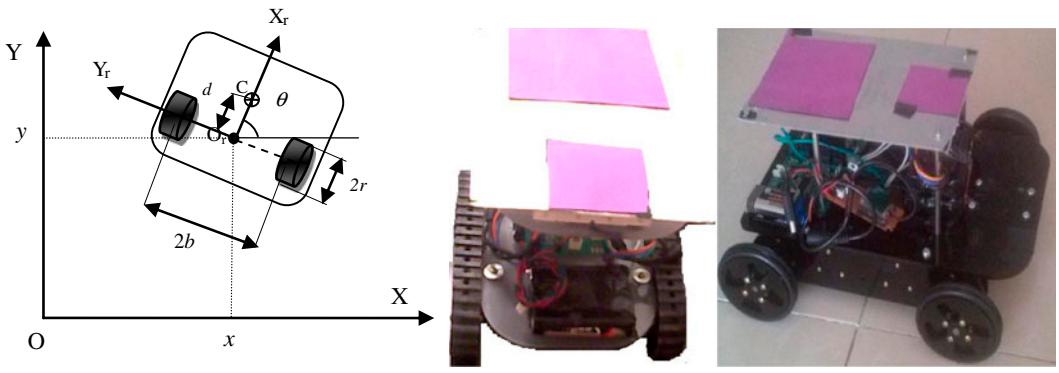


Figure 1. Schematic top view of nonholonomic wheeled mobile robot.

and fuzzy logic to overcome uncertainties in control design for mobile robots. Function approximation methods were also widely used by researchers to compensate uncertainties in different control applications. Function approximation for uncertainty compensation was used in control approaches such as adaptive sliding mode control of hydraulic suspension,[20] adaptive neural compensator of mobile robot trajectory tracking,[21] and adaptive fuzzy neural network control of a robot manipulator, are to name a few. Among the algorithms used for function approximation by fuzzy systems, the gradient descent algorithm is very simple and powerful. To implement this algorithm, however, the value of unknown function in some points should be known.[22] To solve this problem, this paper presents a novel gradient descent algorithm which employs the tracking error instead of the data as input–output pairs for the unknown function. The proposed robust control is superior to the conventional robust control due to the following reasons. One of the most challenging problems in designing a robust controller is to employ an uncertainty bound parameter which should be known in advance or estimated. The value of uncertainty bound parameter is very crucial. Overestimation of this parameter will result in saturation of input and higher frequency of chattering in the switching control laws, while underestimation will increase the tracking error.[23]

This paper uses the voltage control strategy in designing the input–output feedback controller. The voltage control strategy simplifies the control design to be free from the robot dynamics and improves the precision by taking the dynamics of motors into account.[11] This control strategy was originally proposed for robot manipulators in [11] and then was developed for mobile robots.[12] Novel adaptive fuzzy compensator is designed using gradient descent for adjusting the fuzzy system. Advantages of the proposed control design are simplicity in design, fast in response, robustness against uncertainties, deserving guaranteed stability, and precise control performance. In addition, considering actuator dynamics and robot dynamics in an integrated system makes the proposed method more practical. Although the tracking error and its first derivative are the only feedbacks that are used in the control system, the experimental and simulation results show the cogent performance of the proposed controller. Furthermore, the control approach is verified by stability analysis. A comparison with an adaptive feedback linearizing control approach [18] is presented.

The paper is organized as follows. Section 2 presents the dynamics of an electrically driven nonholonomic wheeled mobile robot. Section 3 develops the voltage control of uncertain nonholonomic mobile robot. Section 4 designs the gradient-based adaptive fuzzy estimator for model uncertainties estimation. Section 5 explains the stability analysis and performance evaluation. Section 6 represents the simulation results and comparison by considering kinematic and dynamic disturbances, then experimental results are shown and finally Section 7 concludes the paper.

## 2. Modeling

Kinematics, dynamics, and actuators modeling are presented for an electrically driven nonholonomic two-wheeled mobile robot. Geometric relationships without considering the role of forces and torques deal with kinematics of robot, while dynamic model shows the relation between motions and forces. Actuator modeling relates the control input to the torque input of the wheels of robot. Consider a nonholonomic mobile robot consists of two active wheels or joints. Each wheel is driven by a permanent magnet dc motor through coupling as shown in Figure 1. $OXY$ is the reference coordinate system and $O_rX_rY_r$ is a coordinate system attached to the robot where its origin is located in the middle between the right and left driving wheels. The position $C$ is the center of mass of the mobile robot. The length $d$ is

the distance from $O_r$ to $C$. The length $2b$ is the distance between the two driving wheels and $r_w$ is the radius of the wheel. The position of the robot in the reference frame is represented by $\mathbf{q} = [x\ y\ \theta]^T$ in which $[x\ y]$ is the position of $O_r$ in the reference frame, and $\theta$ is the heading direction taken counterclockwise from the axis $X_r$ to the axis of $X$. The forward kinematics $f_k$ can be represented by

$$\mathbf{q} = f_k(\boldsymbol{\varphi}) \tag{1}$$

where $\boldsymbol{\varphi} = [\,\varphi_r \quad \varphi_l\,]^T$ represents the angular position of right and left wheels, $\varphi_r$ and $\varphi_l$, respectively. By taking the time derivative of (1), the velocity $\dot{\mathbf{q}}$ in the reference frame is obtained as

$$\dot{\mathbf{q}} = \mathbf{J}(\mathbf{q})\dot{\boldsymbol{\varphi}} \tag{2}$$

where $\frac{\partial f_k(\boldsymbol{\varphi})}{\partial \boldsymbol{\varphi}} = \mathbf{J}(\mathbf{q}) \in R^{2\times 3}$ is the Jacobian matrix expressed as

$$\mathbf{J}(\mathbf{q}) = \frac{r_w}{2}\begin{bmatrix} \cos\theta & \cos\theta \\ \sin\theta & \sin\theta \\ 1/b & -1/b \end{bmatrix} \tag{3}$$

The dynamics of robot is described by [2];

$$\mathbf{M}(\mathbf{q})\ddot{\mathbf{q}} + \mathbf{C}(\mathbf{q},\dot{\mathbf{q}})\dot{\mathbf{q}} + \mathbf{F}(\dot{\mathbf{q}}) + \mathbf{G}(\mathbf{q}) + \boldsymbol{\tau}_d + \mathbf{A}^T(\mathbf{q})\lambda = \mathbf{B}(\mathbf{q})\boldsymbol{\tau} \tag{4}$$

where $\mathbf{M}(\mathbf{q}) \in R^{3\times 3}$ denotes the inertia matrix which is a symmetric and positive definitive matrix. $\mathbf{C}(\mathbf{q},\dot{\mathbf{q}})\dot{\mathbf{q}} \in R^3$ is the vector of centrifugal and Coriolis torques, $\mathbf{G}(\mathbf{q}) \in R^3$ is the vector of gravitational torques, $\mathbf{F}(\dot{\mathbf{q}}) \in R^3$ is the vector of frictions, and $\boldsymbol{\tau}_d \in R^3$ is the disturbance. $\mathbf{B}(\mathbf{q}) \in R^{3\times 2}$ is the matrix which transforms the input torques from the joint space to workspace. $\mathbf{A}(\mathbf{q}) \in R^3$ is the vector associated with constraint, and $\lambda \in R$ is the constraint force.

The nonholonomic constraint of the robot is expressed as

$$\dot{x}\sin\theta - \dot{y}\cos\theta = 0 \tag{5}$$

All the kinematic constraints are assumed to be independent of time such that

$$\mathbf{A}(\mathbf{q})\dot{\mathbf{q}} = \mathbf{0} \tag{6}$$

Consider the velocity vector denoted as $\mathbf{v} = [\,\upsilon \quad \omega\,]^T$ where $\upsilon$ is the linear velocity and $\omega$ is the angular velocity in the reference frame under the nonholonomic constraint of pure rolling and nonslipping. Thus,

$$\dot{\boldsymbol{\varphi}} = \mathbf{T}_\varphi \mathbf{v} \tag{7}$$

where

$$\mathbf{T}_\varphi = \frac{1}{r_w}\begin{bmatrix} 1 & b \\ 1 & -b \end{bmatrix} \tag{8}$$

and

$$\dot{\mathbf{q}} = \mathbf{T}_v \mathbf{v} \tag{9}$$

where

$$\mathbf{T}_v = \begin{bmatrix} \cos\theta & 0 \\ \sin\theta & 0 \\ 0 & 1 \end{bmatrix} \tag{10}$$

It would be more suitable to express the dynamic equations of motion in term of internal velocities. Substituting (9) and its differentiation in Equation (4) and pre-multiplying $\mathbf{T}_v$, one can obtain

$$\bar{\mathbf{M}}(\mathbf{q})\dot{\mathbf{v}} + \bar{\mathbf{C}}(\mathbf{q},\dot{\mathbf{q}})\mathbf{v} + \bar{\mathbf{F}}(\dot{\mathbf{q}}) + \bar{\mathbf{G}}(\mathbf{q}) + \bar{\boldsymbol{\tau}}_d = \bar{\mathbf{B}}(\mathbf{q})\boldsymbol{\tau} \tag{11}$$

where $\bar{\mathbf{M}} = \mathbf{T}_v^T\mathbf{M}\mathbf{T}_v \in R^{2\times 2}$, $\bar{\mathbf{F}} = \mathbf{T}_v^T\mathbf{F} \in R^{2\times 1}$, $\bar{\mathbf{G}} = \mathbf{T}_v^T\mathbf{G} \in R^{2\times 1}$, $\bar{\boldsymbol{\tau}}_d = \mathbf{T}_v^T\boldsymbol{\tau}_d \in R^{2\times 1}$, $\bar{\mathbf{C}} = \mathbf{T}_v^T\left(\mathbf{M}\dot{\mathbf{T}}_v + \mathbf{C}\mathbf{T}_v\right) \in R^{2\times 2}$, $\bar{\mathbf{B}} = \mathbf{T}_v^T\mathbf{B} \in R^{2\times 1}$ and $\mathbf{T}_v^T\mathbf{A}^T(\mathbf{q}) = 0$.

**Property** 1: The matrix $\bar{\mathbf{M}}(\mathbf{q})$ is symmetric and positive definite.

**Property** 2: The matrix $\dot{\bar{\mathbf{M}}}(\mathbf{q}) - 2\bar{\mathbf{C}}(\mathbf{q},\dot{\mathbf{q}})$ is skew symmetric matrix.

The electric motors provide the joint torques via the dynamics

$$\mathbf{J}_m\ddot{\boldsymbol{\varphi}}_m + \mathbf{B}_m\dot{\boldsymbol{\varphi}}_m + \mathbf{r}_g\boldsymbol{\tau}_R = \boldsymbol{\tau}_m \tag{12}$$

where $\boldsymbol{\tau}_m \in \mathbf{R}^2$ is the motor torques and $\boldsymbol{\tau}_R \in \mathbf{R}^2$ is the robot torque, $\mathbf{J}_m$, $\mathbf{B}_m$ and $\mathbf{r}_g$ are the $2\times 2$ diagonal matrices for the motor coefficients, namely the inertia, damping, and reduction gear, respectively. The motor velocities $\dot{\boldsymbol{\varphi}}_m \in \mathbf{R}^2$ and wheel velocities $\dot{\boldsymbol{\varphi}}$ are related through the gears as

$$\dot{\boldsymbol{\varphi}}_m = \mathbf{r}_g^{-1}\dot{\boldsymbol{\varphi}} \tag{13}$$

Substituting (9) and (10) into (12), and using (13) yields to

$$\mathbf{J}_m\mathbf{r}_g^{-1}\mathbf{T}_\varphi\dot{\mathbf{v}} + \mathbf{B}_m\mathbf{r}_g^{-1}\mathbf{T}_\varphi\mathbf{v} + \mathbf{r}_g\boldsymbol{\tau}_R = \boldsymbol{\tau}_m \tag{14}$$

In order to obtain the motor voltages as the inputs of system, the electrical equation of geared permanent magnet dc motors in the matrix form is given by

$$\mathbf{L}_a\dot{\mathbf{I}}_a + \mathbf{R}_a\mathbf{I}_a + \mathbf{K}_b\dot{\boldsymbol{\varphi}}_m + \boldsymbol{\zeta} = \mathbf{U} \tag{15}$$

where $\mathbf{U} \in R^2$ is the motor voltages expressed as $\mathbf{U} = [u_r \quad u_l]^T$ in which $u_r$ and $u_l$ are the voltages of right and left motors, respectively. $\mathbf{I_a} \in R^2$ is the vector of motor currents. $\mathbf{R_a}, \mathbf{L_a}, \mathbf{K_b} \in R^{2\times 2}$ represent diagonal matrices for the coefficients of armature resistance, inductance, and back-emf constant, respectively, and $\boldsymbol{\zeta}$ is the external disturbance.

Substituting (9) and (13) into (15) yields

$$\mathbf{L_a}\dot{\mathbf{I}}_\mathbf{a} + \mathbf{R_a}\mathbf{I_a} + \mathbf{K_b}\mathbf{r_g}^{-1}\mathbf{T}_\varphi\mathbf{v} + \boldsymbol{\zeta} = \mathbf{U} \tag{16}$$

The motor torque vector $\boldsymbol{\tau_m}$ is produced by the motor current vector,

$$\boldsymbol{\tau_m} = \mathbf{K_m}\mathbf{I_a} \tag{17}$$

$\mathbf{K_m} \in R^{2\times 2}$ is the diagonal matrix of the torque constants. Using (4)–(17), the state-space model of the electrically driven mobile robot is then derived as

$$\dot{\mathbf{z}} = \mathbf{f_s}(\mathbf{z}) + \mathbf{bU} \tag{18}$$

where

$$\mathbf{b} = \begin{bmatrix} \mathbf{0}_{5\times 2} \\ \mathbf{L_a}^{-1} \end{bmatrix},\ \mathbf{z} = \begin{bmatrix} \mathbf{q} \\ \mathbf{v} \\ \mathbf{I_a} \end{bmatrix} \text{ and } \mathbf{f_s}(\mathbf{z}) = \begin{bmatrix} \mathbf{f_{s1}} \\ \mathbf{f_{s2}} \\ \mathbf{f_{s3}} \end{bmatrix}$$

and

$$\mathbf{f_{s1}} = \mathbf{T_v}\mathbf{z_2}$$

$$\mathbf{f_{s2}} = \left(\mathbf{J_m}\mathbf{r_g}^{-1}\mathbf{T}_\varphi + \mathbf{r_g}\bar{\mathbf{B}}^{-1}\bar{\mathbf{M}}(\mathbf{z_1})\right)^{-1} \cdot \left[\mathbf{K_m}\mathbf{z_3} - \left(\mathbf{B_m}\mathbf{r_g}^{-1}\mathbf{T}_\varphi + \mathbf{r_g}\bar{\mathbf{B}}^{-1}\bar{\mathbf{C}}(\mathbf{z_1}, \mathbf{z_2})\right)\mathbf{z_2} - \mathbf{r_g}\bar{\mathbf{B}}^{-1}(\bar{\mathbf{F}}(\mathbf{z_2}) + \bar{\mathbf{G}}(\mathbf{z_1}) + \bar{\boldsymbol{\tau}}_\mathbf{d})\right]$$

$$\mathbf{f_{s3}} = -\mathbf{L_a}^{-1}\left(\mathbf{K_b}\mathbf{r_g}^{-1}\mathbf{T}_\varphi\mathbf{z_2} + \mathbf{R_a}\mathbf{z_3} + \boldsymbol{\zeta}\right)$$

The state-space equation (18) shows a coupled nonlinear multivariable system. Complexity of the model has been a serious challenge in the literature of mobile robot modeling and control.

## 3. Feedback linearizing control

In order to find a robust control design for an uncertain mobile robot, this paper presents a novel approach. The actual system is described by a model with two parts; the first part: a nominal model which is known and the second part: a lumped uncertainty to cover external disturbances, parametric errors, and unmodeled dynamics. Therefore, the first part is an input–output feedback linearization control law using the nominal model. The second part is a novel gradient-based adaptive fuzzy estimator which estimates the lumped uncertainty.

Let us define output vector $\mathbf{Y}$ as

$$\mathbf{Y} = [x + \alpha\cos\theta \quad y + \alpha\sin\theta]^T \tag{19}$$

where $\alpha$ is the positive small value. $\dot{\mathbf{Y}}$ is calculated by

$$\dot{\mathbf{Y}} = \boldsymbol{\Lambda}\mathbf{v} \tag{20}$$

where

$$\boldsymbol{\Lambda} = \begin{bmatrix} \cos\theta & -\alpha\sin\theta \\ \sin\theta & \alpha\cos\theta \end{bmatrix} \tag{21}$$

The objective of controller is to follow the desired path $\mathbf{q_d}$ where

$$\mathbf{q_d} = [x_d \quad y_d \quad \theta_d]^T \tag{22}$$

$[x_d \quad y_d]$ is the desired $[x\,y]$ and $\theta_d$ is the desired $\theta$. Therefore, the desired output vector $\mathbf{Y_d}$ is defined as:

$$\mathbf{Y_d} = [x_d + \alpha\cos\theta_d \quad y_d + \alpha\sin\theta_d]^T \tag{23}$$

Substituting (20) into (16) yields

$$\mathbf{L_a}\dot{\mathbf{I}}_\mathbf{a} + \mathbf{R_a}\mathbf{I_a} + \mathbf{K}\boldsymbol{\Lambda}^{-1}\dot{\mathbf{Y}} + \boldsymbol{\zeta} = \mathbf{U} \tag{24}$$

where $\mathbf{K} = \mathbf{K_b}\mathbf{r_g}^{-1}\mathbf{T}_\varphi$.

System (24) can be expressed as

$$\hat{\mathbf{K}}\boldsymbol{\Lambda}^{-1}\dot{\mathbf{Y}} + \boldsymbol{\mu} = \mathbf{U} \tag{25}$$

where $\hat{\mathbf{K}}$ is the nominal value for $\mathbf{K}$, and lumped uncertainty $\boldsymbol{\mu}$ is expressed as,

$$\boldsymbol{\mu} = \mathbf{L_a}\dot{\mathbf{I}}_\mathbf{a} + \mathbf{R_a}\mathbf{I_a} + (\mathbf{K} - \hat{\mathbf{K}})\boldsymbol{\Lambda}^{-1}\dot{\mathbf{Y}} + \boldsymbol{\zeta} \tag{26}$$

In fact, $\boldsymbol{\mu}$ is referred to as the lumped uncertainty that includes external disturbance $\boldsymbol{\zeta}$, parametric uncertainty $(\mathbf{K} - \hat{\mathbf{K}})\boldsymbol{\Lambda}^{-1}\dot{\mathbf{Y}}$, and unmodeled dynamics $\mathbf{L_a}\dot{\mathbf{I}}_\mathbf{a} + \mathbf{R_a}\mathbf{I_a}$. System (25) includes the nominal model and the lumped uncertainty. That is

$$\mathbf{U_n} + \boldsymbol{\mu} = \mathbf{U} \tag{27}$$

where the nominal model is expressed as

$$\hat{\mathbf{K}}\boldsymbol{\Lambda}^{-1}\dot{\mathbf{Y}} = \mathbf{U_n} \tag{28}$$

It is worthy to note that the nominal model (28) is known and the lumped uncertainty $\boldsymbol{\mu}$ is unknown. Using (25), and for protecting motors against over voltage, a control law is proposed as

$$\mathbf{U} = u_{\max}\mathbf{sat}(\mathbf{u}/u_{\max}) \tag{29}$$

where $\mathbf{sat}(\mathbf{u}/u_{\max}) = [\,\mathrm{sat}(u_r/u_{\max}) \quad \mathrm{sat}(u_l/u_{\max})\,]^T$ and $u_{\max}$ is the maximum permitted voltage of motor. The saturation function $\mathrm{sat}(u_j/u_{\max})$ for $j = r, l$ is defined by

$$\mathrm{sat}(u_j/u_{\max}) = \begin{cases} 1 & u_j > u_{\max} \\ u_j/u_{\max} & |u_j| \le u_{\max} \\ -1 & u_j < -u_{\max} \end{cases} \tag{30}$$

Let us define $\mathbf{u}$ in the control law (29),

$$\mathbf{u} = \mathbf{U_n} + \hat{\boldsymbol{\mu}} \tag{31}$$

where $\hat{\boldsymbol{\mu}}$ is the estimate of $\boldsymbol{\mu}$ and $\mathbf{U_n}$ is defined as

$$\mathbf{U_n} = \hat{\mathbf{K}}\boldsymbol{\Lambda}^{-1}\left(\dot{\mathbf{Y}}_\mathbf{d} + \mathbf{k_p}\mathbf{E}\right) \tag{32}$$

where $\mathbf{E} = \mathbf{Y_d} - \mathbf{Y}$ and $\mathbf{k_p}$ is the control gain in the form of the positive diagonal matrix. The proposed control approach is based on the voltage control strategy [11] using a model of motor which is much simpler than a model of mobile robot. As a result, the control law will be free from the robot's dynamics.

By substituting the control law (29) into the system (25), one can write the closed loop system as

$$\hat{\mathbf{K}}\boldsymbol{\Lambda}^{-1}\dot{\mathbf{Y}} + \boldsymbol{\mu} = u_{\max}\mathbf{sat}(\mathbf{u}/u_{\max}) \tag{33}$$

Substituting (31) into (33) and using (32) yields to

$$\hat{\mathbf{K}}\boldsymbol{\Lambda}^{-1}\dot{\mathbf{Y}} + \boldsymbol{\mu} = u_{\max}\mathbf{sat}\left(\left(\hat{\mathbf{K}}\boldsymbol{\Lambda}^{-1}\left(\dot{\mathbf{Y}}_\mathbf{d} + \mathbf{k_p}\mathbf{E}\right) + \hat{\boldsymbol{\mu}}\right)/u_{\max}\right) \tag{34}$$

This paper calculates $\hat{\boldsymbol{\mu}}$ by an adaptive fuzzy. The nominal parameter $\hat{\mathbf{K}}$ is known with our knowledge about the parameters. The desired path $\mathbf{Y_d}$ and $\dot{\mathbf{Y}}_\mathbf{d}$ are already defined. The control system is represented in Figure 2.

## 4. Gradient-based adaptive fuzzy uncertainty estimator

Fuzzy systems have been widely employed for function approximation based on the universal approximation property of fuzzy systems.[22] Adaptive fuzzy approaches have shown acceptable performances in approximating and compensating of uncertainty because of their high capability of adaptation.[24,25] Among the algorithms used for function approximation by fuzzy systems, the gradient descent algorithm is very simple and powerful. In this paper, a novel adaptive fuzzy estimator based on gradient descent algorithm is used to estimate the lumped uncertainty.

### 4.1. *Estimation out of the area* $|u_j| \le u_{\max}$

From (33),

$$\boldsymbol{\mu} = u_{\max}\mathbf{sat}(\mathbf{u}/u_{\max}) - \hat{\mathbf{K}}\boldsymbol{\Lambda}^{-1}\dot{\mathbf{Y}} \tag{35}$$

One can suggest $\hat{\boldsymbol{\mu}}$ as

$$\hat{\boldsymbol{\mu}} = u_{\max}\mathbf{sat}(\mathbf{u}/u_{\max}) - \hat{\mathbf{K}}\boldsymbol{\Lambda}^{-1}\dot{\mathbf{Y}} \tag{36}$$

As a result, $\boldsymbol{\mu} = \hat{\boldsymbol{\mu}}$. Therefore, the estimation error is zero.

### 4.2. *Estimation in the area* $|u_i| \le u_{\max}$

Using the condition $|u_i| \le u_{\max}$ implies that

$$u_{\max}\mathbf{sat}\left(\left(\hat{\mathbf{K}}\boldsymbol{\Lambda}^{-1}\left(\dot{\mathbf{Y}}_\mathbf{d} + \mathbf{k_p}\mathbf{E}\right) + \hat{\boldsymbol{\mu}}\right)/u_{\max}\right) = \hat{\mathbf{K}}\boldsymbol{\Lambda}^{-1}\left(\dot{\mathbf{Y}}_\mathbf{d} + \mathbf{k_p}\mathbf{E}\right) + \hat{\boldsymbol{\mu}} \tag{37}$$

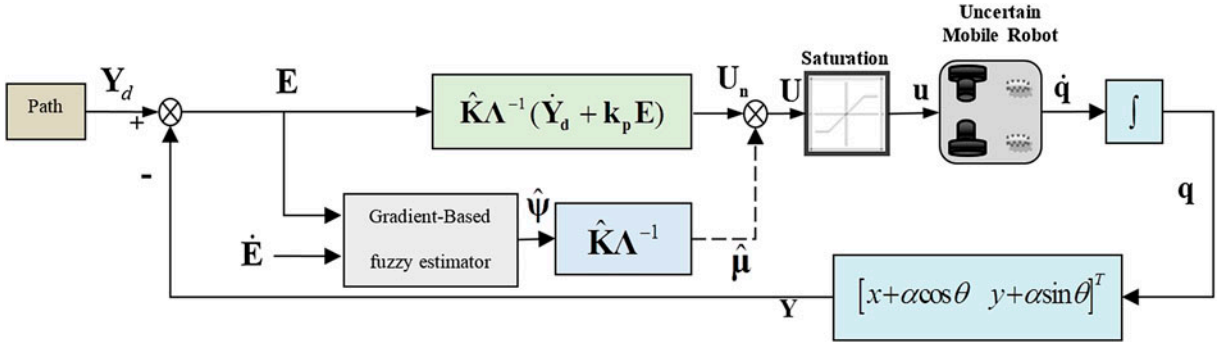


Figure 2. Control system.

Then, the closed loop system (34) is simplified as

$$\dot{\mathbf{E}} + \mathbf{k_p}\mathbf{E} = \mathbf{\Lambda}\hat{\mathbf{K}}^{-1}(\boldsymbol{\mu} - \hat{\boldsymbol{\mu}}) \tag{38}$$

Let us define

$$\boldsymbol{\psi} = \mathbf{\Lambda}\hat{\mathbf{K}}^{-1}\boldsymbol{\mu} \tag{39}$$

$$\hat{\boldsymbol{\psi}} = \mathbf{\Lambda}\hat{\mathbf{K}}^{-1}\hat{\boldsymbol{\mu}} \tag{40}$$

Substituting (40) and (39) into model (38) obtains that

$$\dot{\mathbf{E}} + \mathbf{k_p}\mathbf{E} = \boldsymbol{\psi} - \hat{\boldsymbol{\psi}} \tag{41}$$

Since $\mathbf{k_p}$ is the diagonal matrix, (41) is decoupled as

$$\dot{E}_i + k_{pi}E_i = \psi_i - \hat{\psi}_i \tag{42}$$

where $k_{pi}$ is the $i$th element of the diagonal of $\mathbf{k_p}$ for $i = 1, 2$.

Suppose that $\hat{\psi}_i$ is the output of the decentralized adaptive fuzzy system in the normalized form with the inputs $x_1$ and $x_2$. If three fuzzy sets are given to each input, the whole control space is covered by nine fuzzy rules. The linguistic fuzzy rules are given in Mamdani type

$$\text{FR}_l : \text{If } x_1 \text{ is } A_l \text{ and } x_2 \text{ is } B_l, \quad \text{Then } \hat{\psi}_i \text{ is } C_l \tag{43}$$

where $\text{FR}_l$ denotes the $l$th fuzzy rule for $l = 1, \ldots, 9$. In the $l$th rule, $A_l$, $B_l$, and $C_l$ are fuzzy sets belonging to the fuzzy variables $x_1$, $x_2$, and $\hat{\psi}$, respectively. Three Gaussian membership functions, $\mu_{A_l}(x_1)$, named as positive (P), zero (Z), and negative (N) are defined for the input $x_1$ in the operating range as shown in Figure 3. Three membership functions for $\mu_{B_l}(x_2)$ are defined the same as $\mu_{A_l}(x_1)$. Nine symmetric Gaussian membership functions, $\mu_{C_l}\left(\hat{\psi}_i\right)$, named as very positive high (VPH), positive high (PH), positive medium (PM), positive small (PS), zero (Z), negative small (NS), negative medium (NM), negative high (NH), and very negative high (VNH) are defined for $\hat{\psi}$ in the operating range of output as

$$\mu_l\left(\hat{\psi}_i\right) = \exp\left(-\left(\left(\hat{\psi}_i - \hat{p}_l\right)/\sigma\right)^2\right) \quad \text{for } l = 1, \ldots, 9 \tag{44}$$

The function (44) depends on the parameter $\hat{p}_l$. A gradient-based adaptive law is defined to adjust $\hat{p}_l$. The fuzzy rules should be defined such that the tracking error goes to zero. The obtained fuzzy rules are given in Table 1.

Using the singleton fuzzifier, center average defuzzifier, product inference engine, and Gaussian membership functions, the fuzzy system [17] is of the form

$$\hat{\psi}_i(x_1, x_2) = a/b \tag{45}$$

where $a = \sum_{l=1}^{9} z_l\hat{p}_l$ and $b = \sum_{l=1}^{9} z_l$ where $z_l = \mu_{A_l}(x_1)\mu_{B_l}(x_2)$ that $\mu_{A_l}(x_1) \in [0, 1]$ and $\mu_{B_l}(x_2) \in [0, 1]$ are the membership functions for the fuzzy sets $A_l$ and $B_l$, respectively, and $\hat{p}_l$ is the center of fuzzy set $C_l$. Equation (44) can be represented as

$$\hat{\psi}_i(x_1, x_2) = \sum_{l=1}^{9} \hat{p}_l\eta_l = \hat{\mathbf{p}}^{\mathbf{T}}\boldsymbol{\eta} \tag{46}$$

where $\hat{\mathbf{p}} = [\hat{p}_1 \cdots \hat{p}_9]^T$, $\eta = [\eta_1 \cdots \eta_9]^T$ and $\eta_l$ is the value expressed as

$$\eta_l = z_l/b \tag{47}$$

Using the input scaling factors $k_1$ and $k_2$ to scale $x_1$ and $x_2$, we have

$$x_1 = k_1E \quad \text{and } x_2 = k_2\dot{E} \tag{48}$$

Substituting (48) into (45) describes $\hat{\psi}$ as a function of $E$ and $\dot{E}$ given by

$$\hat{\psi}_i\left(E, \dot{E}\right) = \frac{\sum_{l=1}^{9} \mu_{A_l}(k_1E)\mu_{B_l}\left(k_2\dot{E}\right)\hat{p}_l}{\sum_{l=1}^{9} \mu_{A_l}(k_1E)\mu_{B_l}\left(k_2\dot{E}\right)} \tag{49}$$

Substituting (49) into the closed-loop system (42) yields

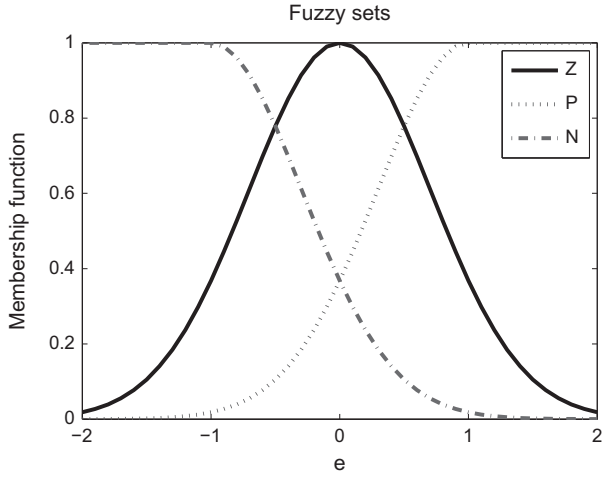


Figure 3. Membership functions of the input.

Table 1. Fuzzy rules.

| $\hat{\psi}_i$ | | $x_2$ | | |
|---|---|---|---|---|
| | | N | Z | P |
| $x_1$ | P | Z | PM | VPH |
| | Z | NS | Z | PS |
| | N | VNH | NM | Z |

$$\psi_i = \dot{E} + k_p E + \hat{\psi}_i(E, \dot{E}) \tag{50}$$

Thus, $\psi_i$ is the function of $E$ and $\dot{E}$ as described by (50). The fuzzy system $\hat{\psi}_i(E, \dot{E})$ in (49) can approximate $\psi_i$ in (51) based on the universal approximation theorem. In order to calculate $\hat{\psi}_i$, let us define a positive function $J_e$ that is the square of estimation error,

$$J_e = 0.5\left(\hat{\psi}_i - \psi_i\right)^2 \tag{51}$$

Therefore, $J_e$ decreases while $\dot{J}_e < 0$ and converge to zero. As a result, $\hat{\psi}_i \to \psi_i$ or the estimation error will become ignorable. In order to have $\dot{J}_e < 0$, it is suggested that

$$\dot{J}_e = -\gamma J_e \tag{52}$$

where $\gamma$ is the positive constant value. As long as $J_e \neq 0$, $\dot{J}_e < 0$. One can calculate $\dot{J}_e$ as

$$\begin{aligned} \dot{J}_e &= \frac{\partial J_e}{\partial \hat{\psi}_i}\frac{\partial \hat{\psi}_i}{\partial a}\frac{\partial a}{\partial \hat{p}_l}\dot{\hat{p}}_l \\ &= \frac{\left(\hat{\psi}_i - \psi_i\right) z_l}{b}\dot{\hat{p}}_l \end{aligned} \tag{53}$$

where $\frac{\partial J_e}{\partial \hat{\psi}_i} = \hat{\psi}_i - \psi_i$, $\frac{\partial \hat{\psi}_i}{\partial a} = \frac{1}{b}$, and $\frac{\partial a}{\partial \hat{p}_l} = z_l$. Value of $z_l$ and $b$ is available, whereas $\hat{\psi}_i - \psi_i$ cannot be computed since $\psi_i$ is uncertain. In order to compute $\hat{\psi}_i - \psi_i$, it is suggested to consider (50) which obtains that

$$\left(\hat{\psi}_i - \psi_i\right) = -\left(\dot{E} + k_p E\right) \tag{54}$$

By substituting (54), (53) in (52), the adaptive law can be written as

$$\dot{\hat{p}}_l = \gamma\left(\dot{E} + k_p E\right) b / z_l \tag{55}$$

Thus,

$$\hat{p}_l = \hat{p}_l(0) + \gamma \int_0^t \left(\left(\dot{E} + k_p E\right) b / z_l\right) \mathrm{d}t' \tag{56}$$

Solving the differential equation (54) results in

$$E = E(0)e^{-k_p t} + \frac{1}{k_p}\int_0^t \left(\psi_i(t') - \hat{\psi}_i(t')\right) e^{-k_p(t-t')} \mathrm{d}t' \tag{57}$$

Since $\psi_i(t') - \hat{\psi}_i(t') \to 0$, $E \to 0$ as $t \to \infty$.

The proposed adaptive fuzzy estimator is based on the gradient decent technique as explained above. The estimator can effectively estimate the uncertainty since the estimation error converges to zero. In addition, the tracking error, $E$, asymptotically converges to zero as expressed by (57). As a novelty, the proposed approach using $\dot{E} + k_p E$ as the estimation error of uncertainty provides that both the estimation error and tracking error converge to zero. Since $\dot{E} + k_p E \to 0$ and $E \to 0$, $\dot{E} \to 0$.

## 5. Stability analysis of the robotic system

The stability of the closed loop system is proven under the following assumptions:

To make the dynamics of the tracking error well defined such that the robot can track the desired path, the following assumption is necessary.

**Assumption 1** The desired path $\mathbf{Y_d}$ must be smooth in the sense that $\mathbf{Y_d}$ and its derivatives up to a necessary order are available and all uniformly bounded.

**Assumption 2** The external disturbance $\boldsymbol{\zeta}$ is bounded as $\|\boldsymbol{\zeta}\| \leq \boldsymbol{\zeta}_{\max}$ where $\boldsymbol{\zeta}_{\max}$ is the positive constant.

The proposed control law (29) obtains a bounded input for every motor that $|u_j| \leq u_{\max}$.

As verified in [12], since the input $u_j$ and the external disturbance $\boldsymbol{\zeta}$ is bounded for each motor, the motor velocity $\dot{\boldsymbol{\varphi}}_{\mathbf{m}}$, the motor current $\mathbf{I_a}$, and its derivative $\dot{\mathbf{I}}_{\mathbf{a}}$ are bonded.

Using $\mathbf{Y_d}$ in (23), we have $\dot{\mathbf{Y}}_{\mathbf{d}} = \begin{bmatrix} \dot{x}_d - \alpha\dot{\theta}_d \sin\theta_d & \dot{y}_d + \alpha\dot{\theta}_d \cos\theta_d \end{bmatrix}^T$. Assumption 1 implies that $\mathbf{Y_d}$ and $\dot{\mathbf{Y}}_{\mathbf{d}}$ are bounded. We have $\mathbf{Y} = \mathbf{Y_d} - \mathbf{E}$ and $\dot{\mathbf{Y}} = \dot{\mathbf{Y}}_{\mathbf{d}} - \dot{\mathbf{E}}$. As proven in Section 4, $E \to 0$ and $\dot{E} \to 0$. Therefore, $\mathbf{Y}$ and $\dot{\mathbf{Y}}$ are bounded and converge to $\mathbf{Y_d}$ and $\dot{\mathbf{Y}}_{\mathbf{d}}$, respectively.

From (20) and (21), $\mathbf{v} = \boldsymbol{\Lambda}^{-1}\dot{\mathbf{Y}}$ where

$$\mathbf{\Lambda}^{-1} = \frac{1}{\alpha}\begin{bmatrix} \alpha\cos\theta & \alpha\sin\theta \\ -\sin\theta & \cos\theta \end{bmatrix} \tag{58}$$

That is a bounded matrix. Since $\dot{\mathbf{Y}}$ is bounded, $\mathbf{v}$ is bounded.

Using (2), (6), (7), and (20), one can obtain that $\dot{\mathbf{q}} = \mathbf{J}(\mathbf{q})\mathbf{T}_{\varphi}\mathbf{\Lambda}^{-1}\dot{\mathbf{Y}}$. Thus,

$$\mathbf{q} = \int_{\mathbf{Y}(0)}^{\mathbf{Y}} \mathbf{J}(\mathbf{q})\mathbf{T}_{\varphi}\Lambda^{-1}\mathbf{d}\boldsymbol{\delta} + \mathbf{q}(0) \tag{59}$$

$\mathbf{J}(\mathbf{q})\mathbf{T}_{\varphi}\mathbf{\Lambda}^{-1}$ is calculated from (2), (6), and (58) as

$$\mathbf{J}(\mathbf{q})\mathbf{T}_{\varphi}\Lambda^{-1} = \begin{bmatrix} \cos^2\theta & \sin\theta\cos\theta \\ \sin\theta\cos\theta & \sin^2\theta \\ -(1/\alpha)\sin\theta & (1/\alpha)\cos\theta \end{bmatrix} \tag{60}$$

Since $\mathbf{Y}$ and $\mathbf{J}(\mathbf{q})\mathbf{T}_{\varphi}\mathbf{\Lambda}^{-1}$ are bounded, $\mathbf{q}$ as expressed in (60) is bounded. Since $\mathbf{J}(\mathbf{q})\mathbf{T}_{\varphi}\mathbf{\Lambda}^{-1}$ is continuous $\mathbf{q} \to \mathbf{q_d}$ as $\mathbf{Y} \to \mathbf{Y_d}$. It was proven that the system states $\mathbf{q}$, $\mathbf{v}$, and $\mathbf{I_a}$ are bounded. Thus, the control system is stable.

## 6. Simulation and experimental results

### 6.1. Simulation

The proposed robust control is simulated according to the model (18) and the controller (34). The frictional torque is given as viscous and coulomb by $\mathbf{F}(\dot{\mathbf{q}}) = 5\dot{\mathbf{q}} + 0.5\text{sign}(\dot{\mathbf{q}})$. The motor and robot parameters are in Table 2. The maximum voltage of motors is set to $u_{\max} = 24\,V$. The nominal parameters are assumed to be 50% of the real values. The external disturbance is $\boldsymbol{\zeta} = [-2 \quad 2]^T$ if $T/4 < t < T/2$ otherwise 0, where $T$ is the total value of the simulation time. The slippage is modeled as a kinematic disturbance [18,26] as $\dot{\mathbf{q}} = \mathbf{T_v}\mathbf{v} + \rho_d[f_{sx} \quad f_{sy} \quad f_s]^T$ where $\rho_d$ is the constant value and $f_{si}$ is the slippage function for $i = x, y, \theta$. $\rho_d = 0.1$ if $T/4 < t < T/2$ otherwise $\rho_d = 0.1$. The proposed method is simulated for set-point and rectangular path tracking. The proposed method is compared with the adaptive feedback linearizing [18] and a voltage-based controller like the proposed controller when the adaptive fuzzy compensator is neglected.

Table 2. Parameters of the motors and robot.

| $r_g$ | $R_a$ (Ω) | $L_a$ (mH) | $K_m$ (Nm/A) | $K_b$ |
|---|---|---|---|---|
| 0.05 | 0.57 | 0.21 | 0.57 | $K_m$ |
| $b$ (m) | $d$ (m) | $I$ (kg m$^2$) | $m_c$ (kg) | $r_w$ (m) |
| 0.265 | 0.1 | 8 | 32 | 0.125 |

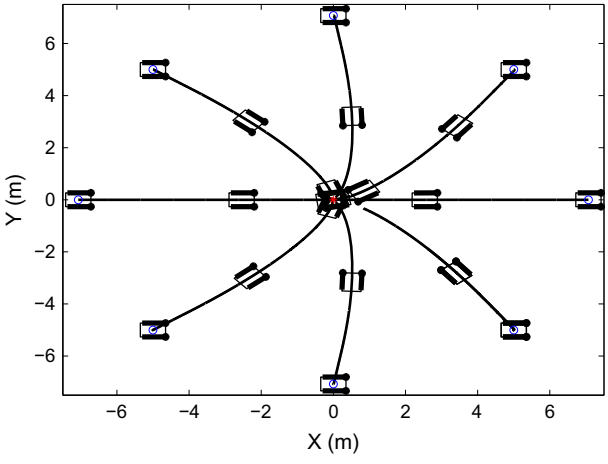


Figure 4. Set-point performance for different initial points.

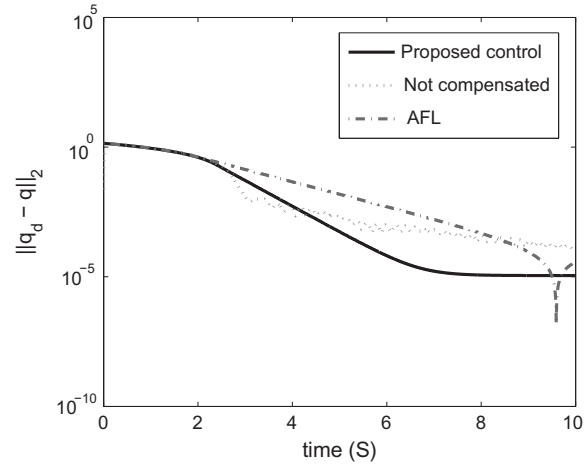


Figure 5. Set-point performances.

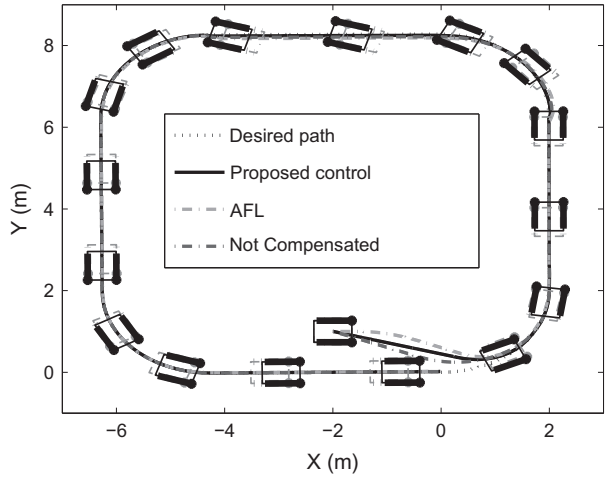


Figure 6. Control performance.

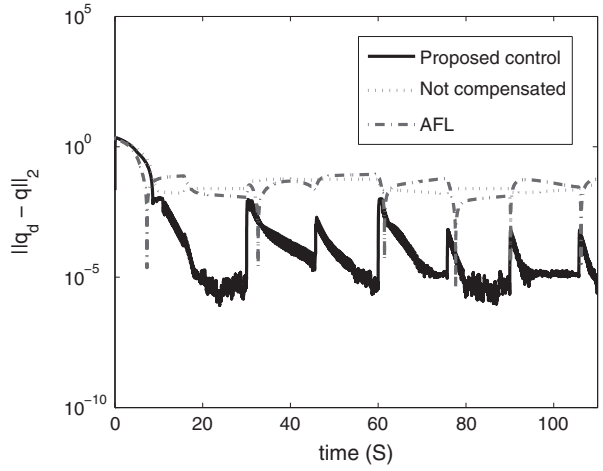


Figure 7. Tracking performances.

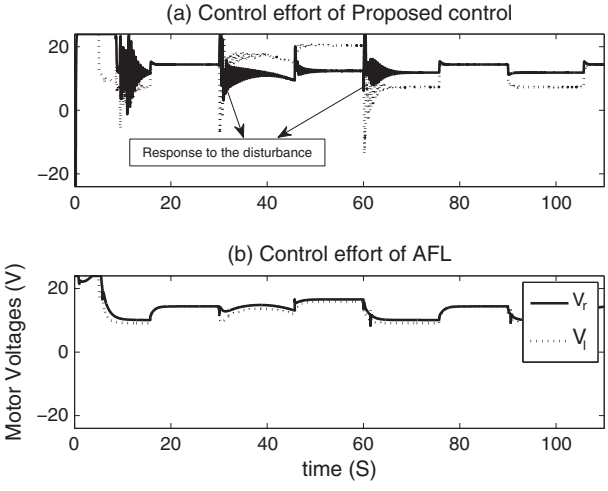


Figure 8. Voltages of motors.

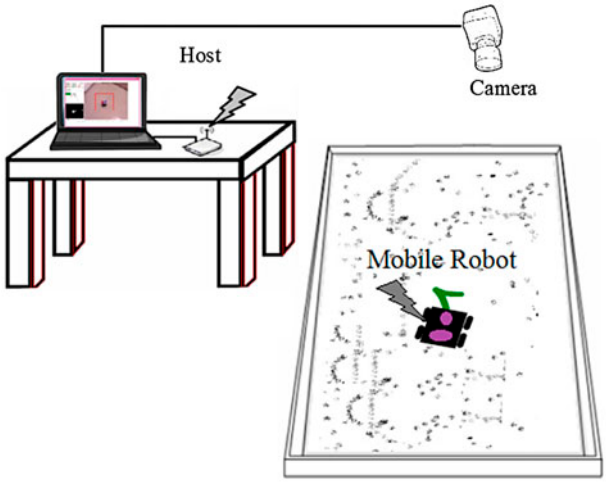


Figure 9. Experimental setup.

The parameters $k_1$ and $k_2$ in (44), $\gamma$ in (54), and $\alpha$ in (20) are set to 1, 1, 10, and 0.05, respectively, and the controller gain is selected as $\mathbf{k_p} = 10I_2$.

### 6.1.1. *Set-point*

The initial tracking error is given as $\|\mathbf{q_d}(0) - \mathbf{q}(0)\|_2 = 5\sqrt{2}$. The set-point problem is evaluated from different initial points, which are shown with small circle and the goal is shown with small star at [0, 0], as shown in Figure 4. The dynamics of errors is satisfactory as shown in Figure 5. The norm of tracking error after 6$S$ converges asymptotically to ignorable value of about $1e-5$.

### 6.1.2. *Tracking*

A comparison between the proposed control and the AFL is presented for tracking of a rectangular path as is depicted in Figure 6. The tracking performance of the proposed control is superior to the AFL control as shown in Figure 7. The norm of tracking error in the proposed control is reduced to $5 \times 10^{-4}$, whereas the norm of tracking error in the AFL control is reduced to $1 \times 10^{-2}$ that is 20 times larger than its value in the proposed control. The control efforts of the proposed controller are shown in Figure 8(a) and AFL voltages are shown in Figure 8(b). The robustness of the proposed controller is obvious because the controller compensates the external disturbances as they are applied to the robot. It is worthy to note that the proposed control is truly less computational than the AFL [19] control, as well. The proposed control is free from the robot dynamics, whereas the AFL and other robust methods [1–9] are dependent on the robot dynamics. In addition, the AFL has ignored the electrical dynamics of motors in the modeling.

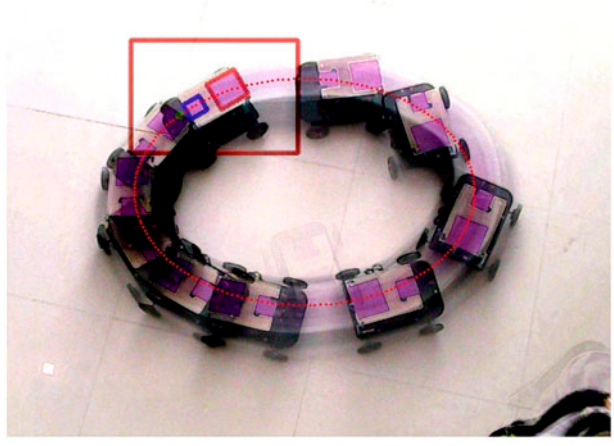

Figure 10. Experimental result for robot 1.

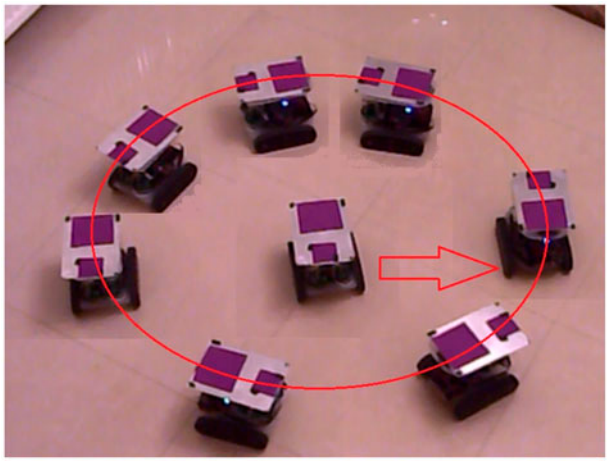

Figure 11. Experimental result for robot 2.

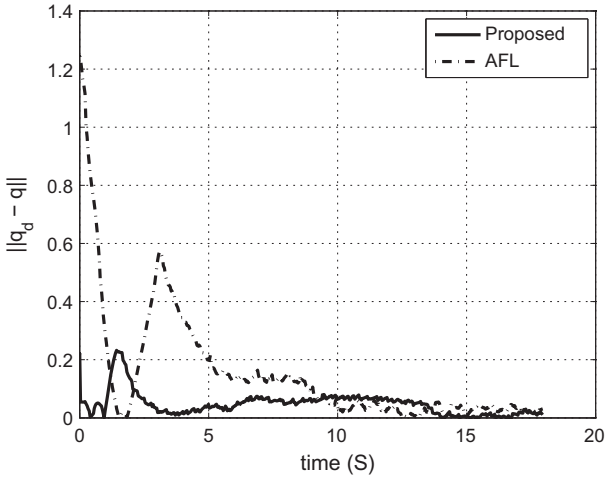


Figure 12. Experimental tracking performance.

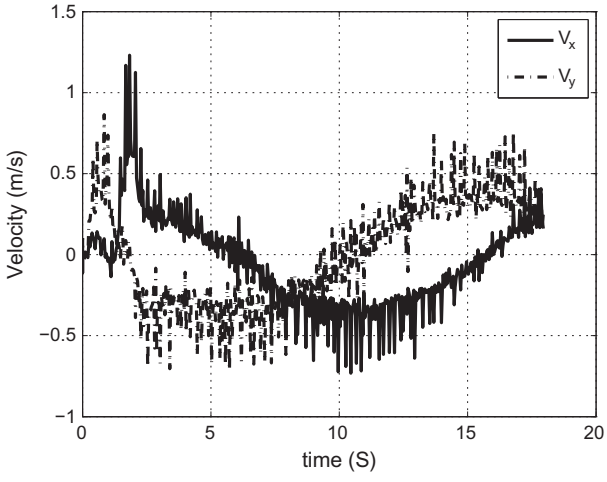


Figure 13. Velocity of the robot for Figure 10.

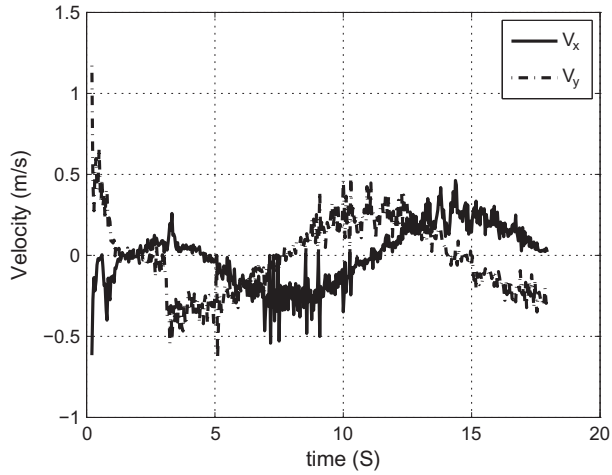


Figure 14. Velocity of the robot for Figure 11.

### 6.2. *Experimental results*

The experimental setup is presented in Figure 9. Proposed robust controller is tested experimentally for circular path tracking by two different low-cost mobile robots to show the performance and being model-free of the proposed controller. The specification of the host computer adopted here is the Intel Core-i5 CPU 2.60 GHz with 4G RAM. The equipment for the experiments is listed as follows: a camera with 640 × 480 resolution, a 2.4 GHz frequency wireless X-Bee radio module that connected the host computer and the mobile robot. The mobile robot consists of the PIC-based driver board, permanent magnet DC motors, gearboxes, receiver, and structural mechanism. A software is developed using Microsoft visual studio 2012 C# for image processing, communicating, and controlling. In this experiment as shown in Figures 10 and 11, the desired path is counterclockwise circle and desired path is red line.

Figure 12 presents the tracking ability of the proposed controller for two different robots in experimental tests. The velocity of robots is represented in the Figures 13 and 14. The velocity profile for the circular path should be sinusoids; however, the measurement noise makes it difficult to see.

## 7. Conclusion

Despite previous complicated robust controllers, this paper has designed a novel model-free and uncomplicated controller for an uncertain wheeled mobile robot using an adaptive fuzzy estimator of uncertainty. The proposed estimation approach has used a novel gradient decent algorithm. This algorithm has been able to minimize the estimation error without using any data for the model uncertainty. Using the tracking error and its first time derivative to form the estimation error of uncertainty, both

the estimation error and tracking error have converged to ignorable values. The proposed control approach has advantages such as simplicity in design, robustness against uncertainties, guaranteed stability, and such as precise control performance. The stability analysis has proven that the proposed control design can guarantee stability, overcome uncertainties, and obtain a good tracking performance in the sense that the tracking error converges asymptotically to ignorable value as illustrated by simulations and experimental tests. A comparison with an adaptive feedback linearizing control approach confirms the superiority of the proposed approach in terms of the precision, simplicity of design, and computations.

## Notes on contributors

**Aliasghar Arab** received his BSc degree in Robotics Engineering in 2011 and his MSc degree in Electrical Engineering in 2013 from Shahrood University of Technology. Currently, he is a visiting researcher with the Department of Mechanical and Aerospace Engineering, Rutgers University, Piscataway, NJ. His current research interests include intelligence and control of the systems, robotic, artificial intelligence, and machine vision.

**Mohammad Mehdi Fateh** received his BSc degree from Isfahan University of Technology in 1988 and his MSc degree in Electrical Engineering from Tarbiat Modares University, Iran, in 1991. He received his PhD degree in Robotic Engineering from Southampton University, UK, in 2001. He is a full professor with the Department of Electrical and Robotic Engineering at University of Shahrood in Iran. His research interests include robust nonlinear control, fuzzy control, robotics, and intelligent systems, mechatronics, and automation.

## References


[1] Chen H, Ma MM, Wang H, et al. Moving horizon $H_\infty$ tracking control of wheeled mobile robots with actuator saturation. IEEE Trans. Control Syst. Technol. 2009;17:449–457.

[2] Yang JM, Kim JH. Sliding mode control for trajectory tracking of nonholonomic wheeled mobile robots. IEEE Trans. Rob. Autom. 1999;15:578–587.

[3] Fukao T, Nakagawa H, Adachi N. Adaptive tracking control of a nonholonomic mobile robot. IEEE Trans. Neural Networks. 2000;16:609–615.

[4] Chen C, Li TS, Yeh Y, et al. Design and implementation of an adaptive sliding-mode dynamic controller for wheeled mobile robots. Mechatronics. 2009;19:156–166.

[5] Hwang EJ, Kang HS, Hyun CH, et al. Robust backstepping control based on a Lyapunov redesign for skid-steered wheeled mobile robots. Int. J. Adv. Rob. Syst. 2013;10:1–8.

[6] Ma BL, Tso SK. Robust discontinuous exponential regulation of dynamic nonholonomic wheeled mobile robots with parameter uncertainties. Int. J. Robust Nonlinear Control. 2008;18:960–974.

[7] Kim MS, Shin JH, Hong SG, et al. Designing a robust adaptive dynamic controller for nonholonomic mobile robots under modeling uncertainty and disturbances. Mechatronics. 2003;13:507–519.

[8] Mohareri O, Dhaouadi R, Rad AB. Indirect adaptive tracking control of a nonholonomic mobile robot via neural networks. Neurocomputing. 2012;88:54–66.

[9] Das T, Kar IN. Design and implementation of an adaptive fuzzy logic-based controller for wheeled mobile robots. IEEE Trans. Control Syst. Technol. 2006;14:501–510.

[10] Su KH, Chen YY, Su SF. Design of neural-fuzzy-based controller for two autonomously driven wheeled robot. Neurocomputing. 2010;73:2478–2488.

[11] Fateh MM. On the voltage-based control of robot manipulators. Int. J. Control Autom. Syst. 2008;6:702–712.

[12] Fateh MM, Arab A. Robust control of a wheeled mobile robot by voltage control strategy. Nonlinear Dyn. 2014. Published online. doi:10.1007/s11071-014-1667-8.

[13] Oriolo G, De Luca A, Vendittelli M. WMR control via dynamic feedback linearization: design, implementation, and experimental validation. IEEE Trans. Control Syst. Technol. 2002;10:835–852.

[14] Kanayama Y, Kimura Y, Miyazaki F, et al. A stable tracking control method for an autonomous mobile robot. Proc. IEEE Conf. Rob. Autom. 1990;384–389.

[15] Dong W, Xu WL. Adaptive tracking control of uncertain nonholonomic dynamic system. IEEE Trans. Autom. Control. 2001;46:450–454.

[16] Lee TH, Lam HK, Leung FHF, et al. Application notes – a practical fuzzy logic controller for the path tracking of wheeled mobile robots. IEEE Control Syst. Mag. 2003;23:60–65.

[17] Fierro R, Lewis FL. Control of a nonholonomic mobile robot using neural networks. IEEE Trans. Neural Networks. 1998;589–600.

[18] Shojaei K, Mohammad-Shahri A, Tarakameh A. Adaptive feedback linearizing control of nonholonomic wheeled mobile robots in presence of parametric and nonparametric uncertainties. Rob. Comput. Integr. Manuf. 2011;27:194–204.

[19] Hou ZG, Zou AM, Cheng L, et al. Adaptive control of an electrically driven nonholonomic mobile robot via backstepping and fuzzy approach. IEEE Trans. Control Syst. Technol. 2009;17:803–815.

[20] Huang SJ, Chen HY. Adaptive sliding controller with self-tuning fuzzy compensation for vehicle suspension control. Mechatronics. 2006;16:607–622.

[21] Wai RJ, Yang ZW. Adaptive fuzzy neural network control design via a T–S fuzzy model for a robot manipulator including actuator dynamics. IEEE Trans. Syst. Man Cybern. Part B Cybern. 2008;38:1326–1346.

[22] Wang LX. A course in fuzzy systems and control. New York, NY: Prentice-Hall; 1997.

[23] Fateh MM. Proper uncertainty bound parameter to robust control of electrical manipulators using nominal model. Nonlinear Dyn. 2010;61:655–666.

[24] Chiou KC, Huang SJ. An adaptive fuzzy controller for robot manipulators. Mechatronics. 2005;15:151–177.